Seismic Detection and Characterization of the Altiplano-Puna Magma Body, Central Andes

GEORGE ZANDT[1], MARK LEIDIG[1], JOSEF CHMIELOWSKI[1],
DAVID BAUMONT[1] and XIAOHUI YUAN[2]

Abstract — The Altiplano-Puna Volcanic Complex (APVC) in the central Andes is the product of an ignimbrite "flare-up" of world class proportions (DE SILVA, 1989). The region has been the site of large-scale silicic magmatism since 10 Ma, producing 10 major eruptive calderas and edifices, some of which are multiple-eruption resurgent complexes as large as the Yellowstone or Long Valley caldera. Seven PASSCAL broadband seismic stations were operated in the Bolivian portion of the APVC from October 1996 to September 1997 and recorded teleseismic earthquakes and local intermediate-depth events in the subducting Nazca plate. Both teleseismic and local receiver functions were used to delineate the lateral extent of a regionally pervasive ~20-km-deep, very low-velocity layer (VLVL) associated with the APVC. Data from several stations that sample different parts of the northern APVC show large amplitude *Ps* phases from a low-velocity layer with $Vs \leq 1.0$ km/s and a thickness of ~1 km. We believe the crustal VLVL is a regional sill-like magma body, named the Altiplano–Puna magma body (APMB), and is associated with the source region of the Altiplano–Puna Volcanic Complex ignimbrites (CHMIELOWSKI *et al.*, 1999).

Large-amplitude *P–SH* conversions in both the teleseismic and local data appear to originate from the top of the APMB. Using the programs of LEVIN and PARK (1998), we computed synthetic receiver functions for several models of simple layered anisotropic media. Upper-crustal, tilted-axis anisotropy involving both *Vp* and *Vs* can generate a "split *Ps*" phase that, in addition to the *Ps* phase from the bottom of a thin isotropic VLVL, produces an interference waveform that varies with backazimuth. We have forward modeled such an interference pattern at one station with an anisotropy of 15%–20% that dips 45° within a 20-km-thick upper crust. We develop a hypothesis that the crust above the "magma body" is characterized by a strong, tilted-axis, hexagonally symmetric anisotropy. We speculate that the anisotropy is due to aligned, fluid-filled cracks induced by a "normal-faulting" extensional strain field associated with the high elevations of the Andean Puna.

Key words: PASSCAL, receiver functions, anisotropy, magma body, Altiplano-Puna, APVC.

Introduction

The detection and characterization of magma bodies in the crust and upper mantle has been a long-standing goal in seismology, and a topic of interest for Kei Aki throughout his career (e.g., AKI, 1968; AKI *et al.*, 1978; ROBERTS, AKI,

[1] Department of Geosciences, Gould-Simpson Building, University of Arizona, Tucson, Arizona 85721-0077, U.S.A. E-mail: zandt@geo.arizona.edu
[2] GeoForschungsZentrum, Potsdam, Germany.

and FEHLER, 1991). Early studies of magma bodies were often based on the fortuitous observation of "exotic" phases within waveforms recorded in volcanic regions (PEPPIN, 1987). Aki and his colleagues pioneered the formulation of the seismic travel-time inversion technique now commonly called "tomography" (AKI *et al.*, 1977). Among the first targets of the new technique taken up by his students was detection of crustal magma bodies and mantle asthenosphere in Hawaii, Yellowstone, and California (ELLSWORTH and KOYANAGI, 1977; IYER *et al.*, 1981; ZANDT and FURLONG, 1982). IYER (1984) summarized the evidence for the locations, shapes, and sizes of magma bodies beneath regions of Quaternary volcanism based on seismic tomography as well as other geophysical techniques.

The difficulties of geophysical imaging of a crustal magma body are exemplified by the many studies conducted at Long Valley caldera, California (RUNDLE and HILL, 1988). Although a low-velocity zone beneath the caldera had been found as early as 1976 by a teleseismic *P*-wave delay study by STEEPLES and IYER (1976), the precise depth, shape and velocity reduction has been difficult to accurately assess (STECK and PROTHERO, 1994). The difficulties of imaging a magma body are caused by a combination of factors: complex structure in volcanic regions, especially with near-surface heterogeneity, the tendency of seismic waves to refract around low-velocity zones, and strong attenuation and anisotropy effects often associated with magmatic structures in the crust. Among the best-resolved magma chambers are mid-crustal, tabular-shaped bodies exemplified by the Socorro magma body delineated by microearthquake studies (SANDFORD *et al.*, 1973), seismic reflection surveys (BROWN *et al.*, 1980), and converted phase observations (SHEETZ and SCHLUE, 1992; SCHLUE *et al.*, 1996).

In this contribution, we describe another well-constrained observation of a regionally extensive, sill-like magma body at mid-crustal depth. We will present data for the existence of highly developed anisotropy in the upper 20 km of the crust in the Altiplano-Puna Volcanic Complex (APVC), a major silicic volcanic field straddling the political triple junction of Bolivia, Chile, and Argentina (Fig. 1). The anisotropic upper crust appears to be associated with the areal extent of the magma body. The existence of the magma body is based on the observations of large-amplitude, negative-polarity *Ps* phases observed on receiver functions from PASSCAL stations that we had deployed in the APVC during 1996–1997 (CHMIELOWSKI *et al.*, 1999). Matching the large amplitudes of these *Ps* phases requires a $Vs \leq 1$ km/s within a $\sim$1-km-thick layer. A purely isotropic model cannot explain the observation of significant azimuthal variations of the *Ps* amplitude on the radial receiver functions, nor the existence of corresponding large-amplitude phases on the transverse component. Based on preliminary forward modeling of the waveform data, we suggest that the upper crust is characterized by 15%–20% anisotropy with a tilted symmetry axis.
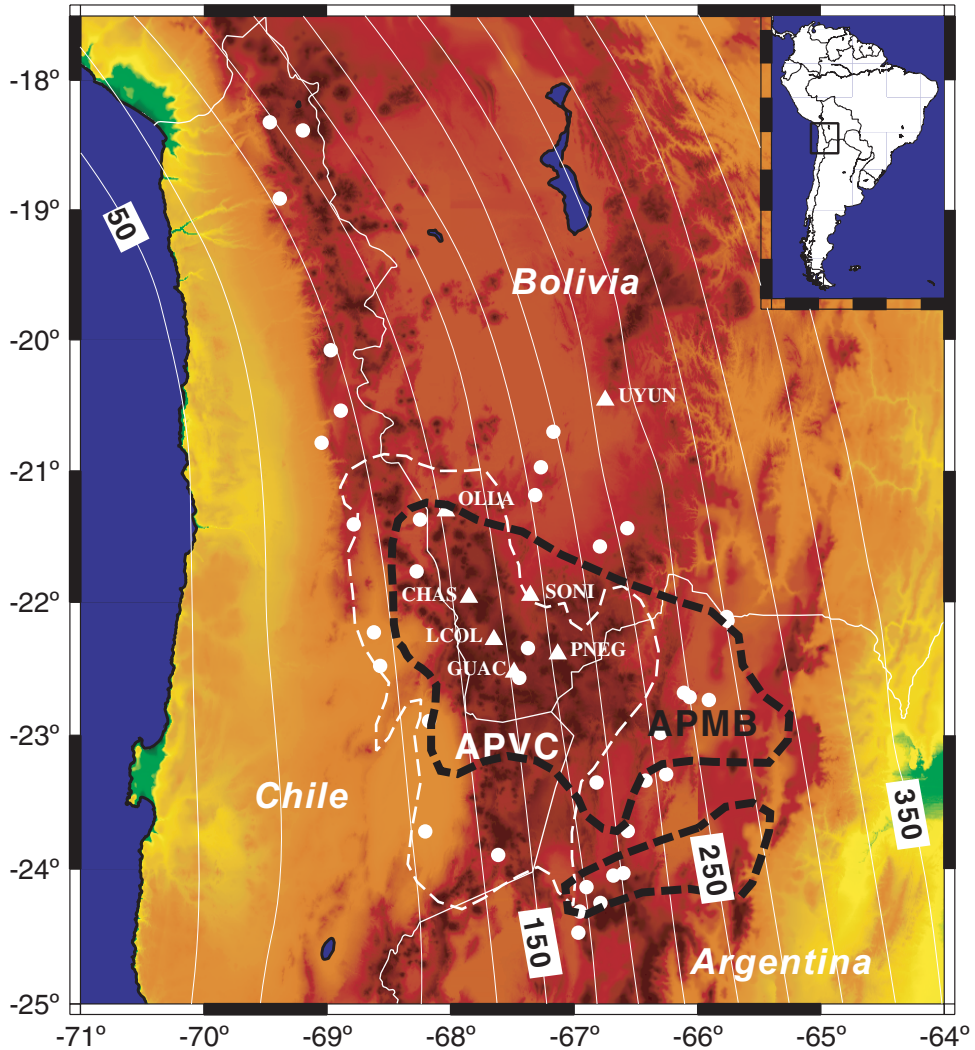
Figure 1

Location map of the Altiplano-Puna Volcanic Complex (APVC, enclosed by the dashed white line) and the one-year deployment of PASSCAL broadband stations (triangles). Dashed black line encloses the approximate extent of the mid-crustal Altiplano-Puna magma body (APMB) determined in this study. Solid circles are epicenters of intermediate-depth earthquakes utilized in this study. Thin lines are the contours of depth (km) to the Wadati-Benioff zone from CAHILL and ISACKS (1992).

APVC Background

Since the late Miocene, an ignimbrite "flare-up" has produced a major silicic volcanic province, the Altiplano–Puna Volcanic Complex (APVC), in the central Andes of South America (DE SILVA, 1989) (Fig. 1). An ignimbrite (or ash-flow tuff) is

a pumice and ash deposit left by pyroclastic flows originating from the collapse of a vesiculated magmatic eruption column (FRANCIS, 1993). The term "flare-up" was first coined for the mid-Tertiary eruptions of the western United States (CONEY, 1972). "Flare-ups" result when large calderas occur in clusters or complexes such that multiple eruptions produce voluminous ignimbrite cover. Examples of large caldera complexes within the United States include the San Juan field in the central Rocky Mountains and the Indian Peak volcanic field in southern Nevada (MAUGHAN *et al.*, 2000). The APVC is a youthful, active analogue of these western U.S. caldera complexes.

Several young ignimbrite fields occur in the Central Volcanic Zone of the central Andes (BAKER, 1981; DE SILVA and FRANCIS, 1991). The Altiplano-Puna volcanic complex is the youngest of these and covers approximately 50,000 km^2 between 21° and 24°S. The APVC constitutes the largest ignimbrite concentration in the Central Volcanic Zone of the Andes (Fig. 1) and one of the largest in the world (DE SILVA, 1989). The APVC is located at the southward transition between the $\sim$4-km-high plateau of the Altiplano and the $\sim$5-km-high Puna, a change that may be associated with a rapid southward thinning of the South American lithosphere (WHITMAN *et al.*, 1996).

The APVC is located 100–250 km above the Nazca plate where it subducts with a relatively uniform $\sim$30° dip (CAHILL and ISACKS, 1992) (Fig. 1). Crustal seismicity levels are very low in the APVC crust, as they are throughout the central Andes, due to the unusually thick and weak crust (BECK *et al.*, 1996; ZANDT *et al.*, 1996; BILLS *et al.*, 1994). However, a concentration of larger-magnitude intermediate-depth earthquakes with focal depths between 150 to 300 km (the Jujuy cluster) is located beneath the eastern margin of the APVC. This cluster of strong earthquakes located almost directly beneath the APVC presents a rare opportunity to probe the lithosphere of a major caldera complex.

Studies of the voluminous ignimbrites by DE SILVA (1989) and others suggest the APVC flare-up is due primarily to crustal melting in response to tectonic crustal thickening associated with the building of the central Andes, with a lesser contribution from subduction-related melts. The region has been the site of large-scale silicic magmatism since 10 Ma, with several major caldera-forming eruptions producing >15,000 km^3 of ignimbrites (DE SILVA, 1989; DE SILVA and FRANCIS, 1991). The APVC ignimbrites are part of a distinct end-member class called the monotonous intermediate type characterized by large volumes of a limited compositional range that probably reflects a pre-eruption evolution in a slab-like magma chamber (MAUGHAN *et al.*, 2000). Late Pleistocene to Recent volcanic activity in the form of large silicic lava flows and domes and two major geothermal fields indicate that the APVC province remains magmatically active (DE SILVA 1989; DE SILVA, *et al.*, 1994).

Discovery of the APMB

Recently we published a study of teleseismic receiver functions for 14 events recorded by seven PASSCAL broadband stations deployed for one year in the northeast portion of the APVC (CHMIELOWSKI *et al.*, 1999). We used the method of receiver functions to probe the crustal stratigraphy. The basis of this technique is that a *P* wave propagating up to a seismic station produces converted *S* waves (*Ps*) at any seismic impedance contrast (e.g., the Moho or a magma body). A teleseismic *P* wave, or a *P* wave generated by a subcrustal local event, is steeply incident and dominates the vertical component of ground motion, whereas the *Ps* conversions are contained mostly on the horizontal components. Receiver functions are seismic waveforms computed by deconvolving the vertical component from the radial component to isolate and highlight the *Ps* converted phases within the coda of the *P* waves (ZANDT *et al.*, 1995). We computed all of our receiver functions, for teleseismic and local events, using a new time-domain, iterative deconvolution algorithm (LIGORRIA and AMMON, 1999). The method entails doing a cross correlation between the vertical and radial components of the seismograms to find the lag and amplitude of the first and largest spike (Gaussian) in the receiver function. Then the current estimate of the receiver function is convolved with the vertical component and subtracted from the radial component, and the procedure is repeated to estimate other spike lags and amplitudes. With each additional spike in the receiver function the misfit between the convolution of the vertical component and the receiver function and the radial component is reduced, and the iteration halts when the misfit falls below a prescribed threshold. Long-period stability is insured *a priori* by construction of the deconvolution as a sum of Gaussian pulses. This method has the advantage of finding the "simplest" receiver function with high-frequency content but without side-lobe artifacts or long-period instability often associated with frequency-domain and some other time-domain techniques.

The teleseismic radial receiver functions for all our stations within the APVC have a large-amplitude, negative-polarity *Ps* conversion at approximately 2.5 s after the direct *P* wave and a smaller positive *Ps* conversion between 3 and 5 s after the direct *P* wave (Fig. 2). We suggested from forward modeling that the first conversion is produced by the top of a very low-velocity layer (VLVL) at a depth of 19 km, and we interpreted the second *Ps* as the bottom of the VLVL. We found the VLVL must have a *Vs* ≤ 1.0 km/s and a thickness of ∼1 km to match the amplitudes and timing from several stations that sample different parts of the northern APVC. We interpreted this crustal VLVL as a regional sill-like magma body associated with the Altiplano–Puna Volcanic Complex, and we named it the Altiplano–Puna magma body (APMB) (CHMIELOWSKI *et al.*, 1999).

To test the resolving capability of relatively long-period receiver functions on thin, crustal low-velocity zones, we computed reflectivity synthetics for a suite of models varying both the thickness and velocity of a low-velocity layer (Fig. 3). The results
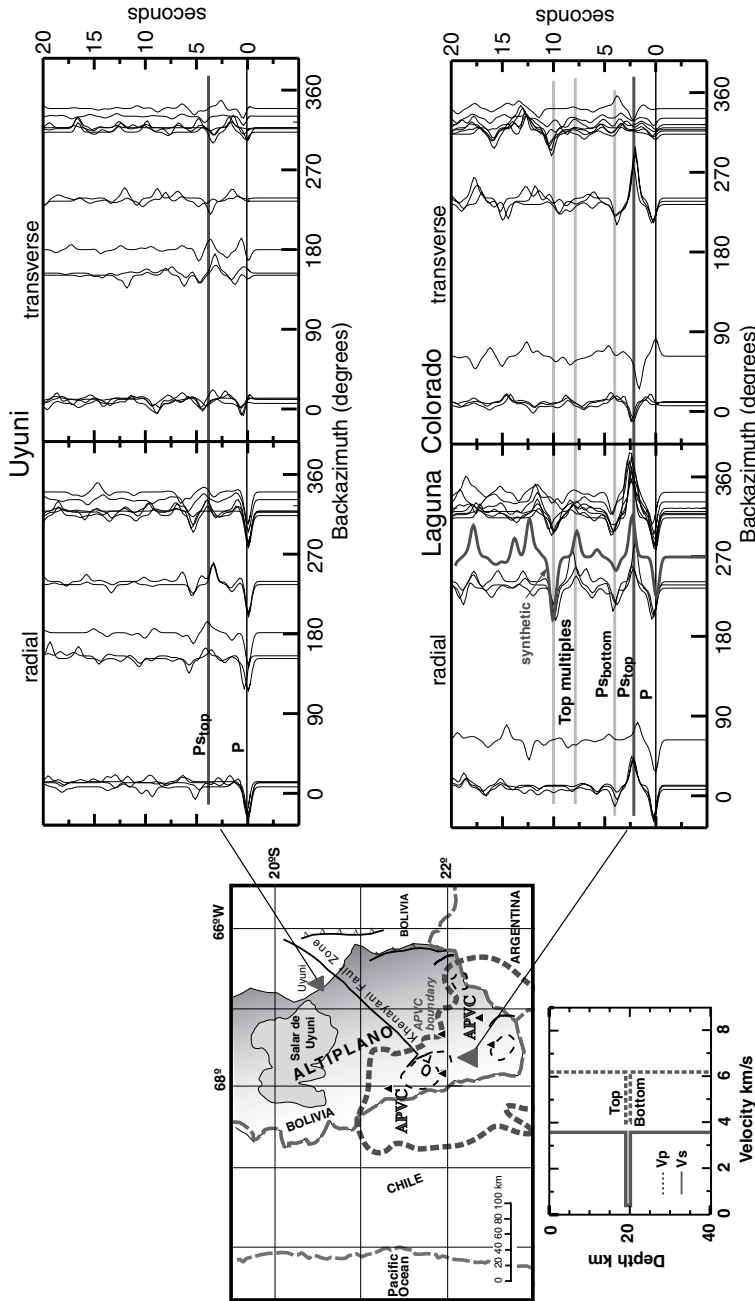
Figure 2

Comparison of teleseismic receiver functions recorded outside the APVC (Uyuni) and within the APVC (Laguna Colorado). The receiver functions at Uyuni are unremarkable except for the evidence of a relatively subdued lower crustal low-velocity zone at a depth of approximately 30–35 km. In contrast, radial receiver functions at Laguna Colorado show a very large amplitude, negative polarity arrival at ~2.5 seconds, consistent with a Ps conversion from the top of a very low-velocity layer at a depth of ~20 km. A synthetic receiver function from a simple model (lower left) with a 1-km-thick layer with Vs ~0.5 km/s can fit the main features of the radial data. However, the variations in the amplitude of the radial Ps phase and the corresponding arrivals on the transverse data showing reversals in polarity cannot be explained by isotropic models but could be explained by the presence of highly developed anisotropy between the converter interface and the surface.
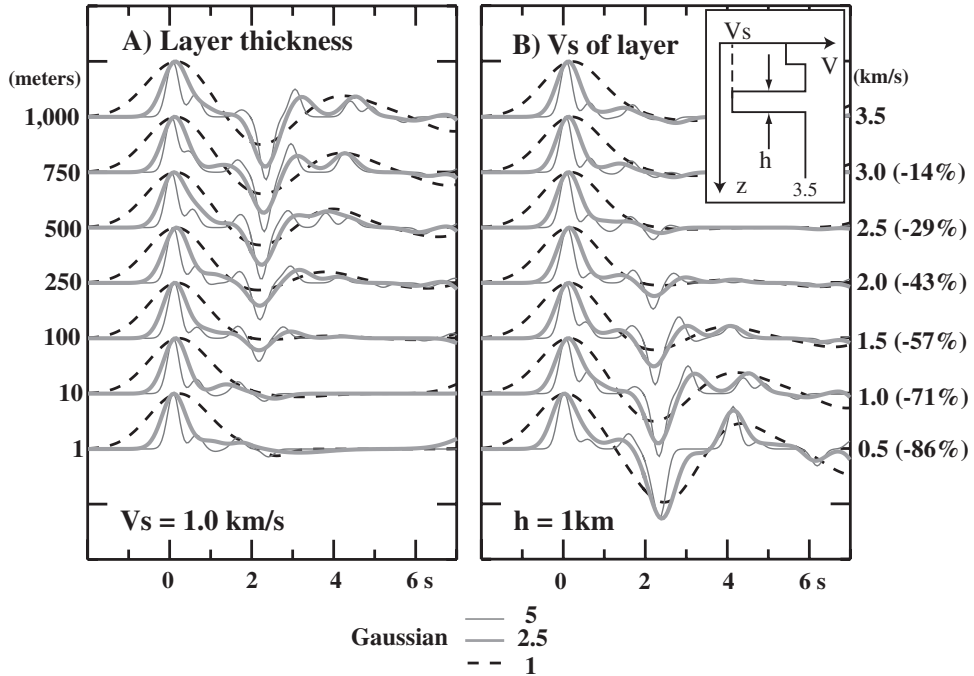
Figure 3

Resolution test for low-velocity-layer (lvl) thickness, h and velocity, Vs as a function of frequency. The three Gaussian widths of 5, 2.5, and 1 correspond to Gaussian low-pass filters with 90% cutoff at frequencies of 2.4, 1.2, and 0.5 Hz, respectively. (A) Synthetic receiver functions for varying lvl thickness with constant velocity of 1 km/s. Note that for Gaussians ≥ 2.5 the lvl is detectable for layers as thin as 100 m, although the full amplitude is not developed until the thickness approaches 1 km. (B) Synthetic receiver functions for varying lvl velocity with constant thickness of 1 km. Note that for Gaussians ≥ 2.5 the lvl is detectable for layers with velocity < ~2 km/s, although the full amplitude is not developed until the velocity approaches 1 km/s.

demonstrate that with a nominal frequency content of an earthquake-source receiver function, a crustal low-velocity layer with $Vs = 1$ km/s can be detected if it is greater than ~100 m thick. The full amplitude is developed as the thickness approaches 1 km. Conversely, a 1-km-thick low-velocity layer is detectable for velocities less than ~2 km/s, and the full amplitude is developed as the velocity approaches 1 km/s. In contrast to the case of travel-time tomography where the ray bending effects of low-velocity zones impede resolution, the low velocity aids resolution of a thin layer by creating greater separation of the converted phases from the top and bottom of the layer.

Lateral Extent of the APMB

Our PASSCAL deployment was largely confined to the northeast portion of the Altiplano–Puna volcanic complex. We were able to greatly expand our analysis to

include most of the APVC using data from the SFB-267 project (Deformazion in den Andes) in cooperation with researchers from the GFZ-Potsdam and Freie University-Berlin. This large multi-year project occupied ∼100 sites with short-period instruments deployed in three separate, overlapping experiments of about 3 months each (Fig. 4). Combining data from the three GFZ-FU deployments, we computed a total of 88 receiver functions using the same processing techniques as in the APVC study (CHMIELOWSKI *et al.*, 1999). The relatively short duration of the deployments limited the number of events available for analysis, however the spatial density and broad coverage of the German instruments was essential in constraining the lateral boundaries of the APMB.

   We considered a receiver function to contain evidence for the APMB if a negative-polarity conversion arrived between 1.5 and 3.0 s after the *P* wave with an amplitude >50% of that of the direct *P* wave. If the amplitude of the *Ps* conversion was between 30% and 50% of that of the direct *P* wave, we considered the presence of the APMB ambiguous. Finally, if the amplitude of the *Ps* conversion was <30% of the direct *P* wave amplitude, or if its timing was not between 1.5 and 3.0 s, we considered the APMB absent beneath the station. The resulting map of the lateral extent of the APMB covers an area about 3° in longitude and about 2° in latitude, or approximately 60,000 km^2.

   An important observation about the APMB is that it most closely correlates with the distribution of the <7 Ma ignimbrite complexes and not with the line of Quaternary arc volcanoes (Fig. 4). This spatial correlation strengthens the argument that this seismic structure is associated with the magmatic plumbing of the APVC and not necessarily with the active arc volcanoes.

Evidence for Strong Anisotropy

A unique advantage in studying the seismic structure of the APVC compared to many other caldera complexes is the presence of a very active Wadati–Benioff zone in the subducting slab (Fig. 1). The subcrustal earthquakes are abundant and many have unusually large magnitudes. We combined global data for the largest events ($M > 5.8$) and many a selection of additional smaller magnitude earthquakes distributed around our APVC network and performed a joint hypocenter relocation on the resulting set of 52 events. From the relocated events, we selected 38 from which to compute receiver functions using the iterative deconvolution technique of LIGORRIA and AMMON (1999). From among the best receiver functions, we stacked those with similar backazimuths for each station.

   After low-pass filtering (corner of 0.9 Hz), the stacked local receiver functions were plotted by back-azimuth with the teleseismic receiver functions. Where we have both teleseismic and local receiver functions for comparable backazimuths, the waveforms are similar, giving us confidence in the fidelity of the local receiver
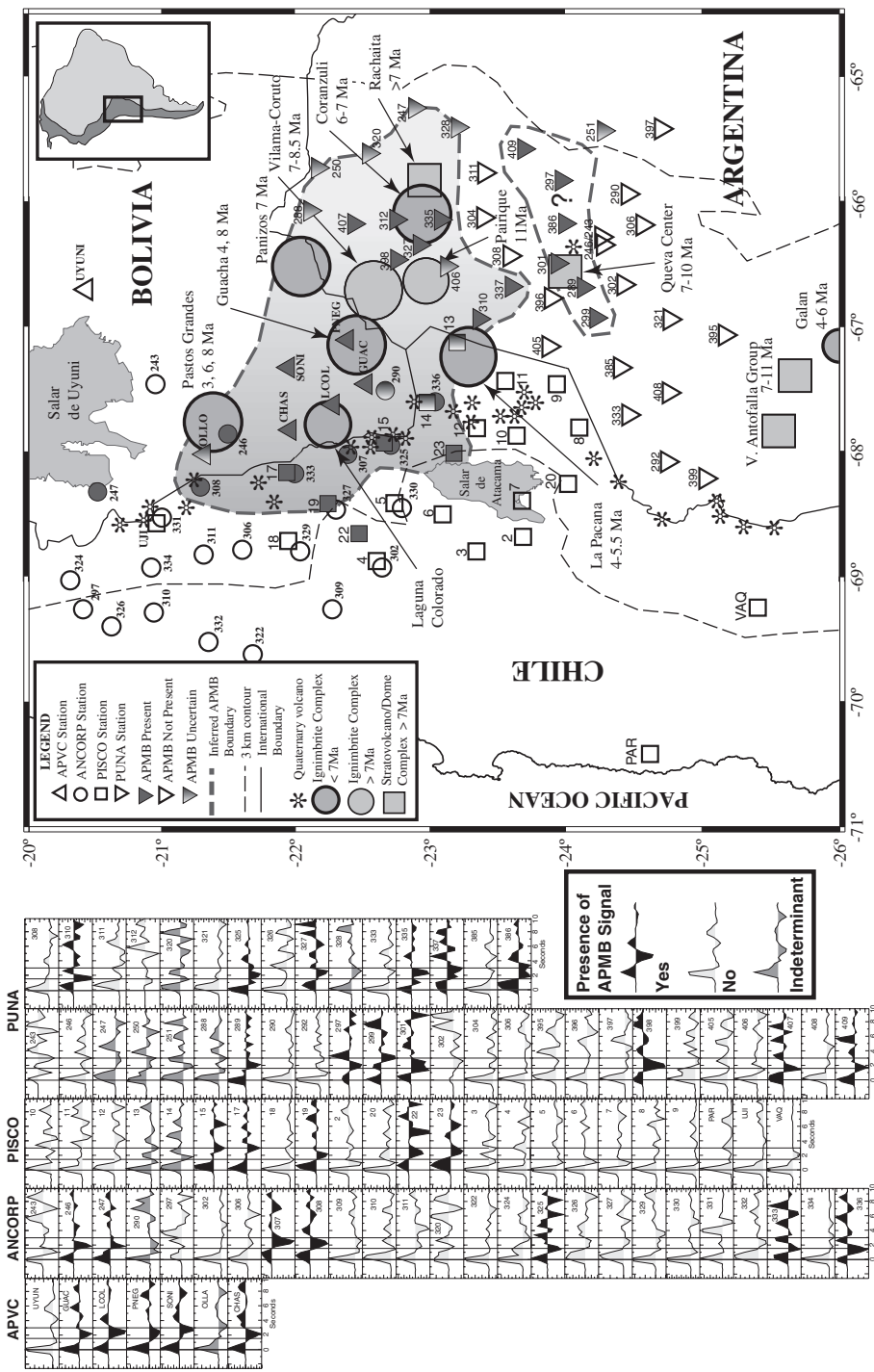
Figure 4

Areal extent of the Altiplano-Puna Magma Body (APMB) as mapped out by large-amplitude *Ps* conversions recorded by stations of the APVC, ANCORP, PISCO, and PUNA deployments. Note that it underlies the high elevations (>3 km) of the Altiplano–Puna transition and correlates most closely with the distribution of the caldera complexes and not with the occurrence of Quaternary volcanoes.

functions (Fig. 5). With the additional coverage from the local receiver functions, significant azimuthal variations in the radial waveform, only hinted at from the teleseismic data, become obvious in the APVC data (Fig. 5a). On the radial receiver functions, the *Ps* from the top of the low-velocity layer exhibits large-amplitude variations and timing perturbations. On the transverse receiver functions the corresponding phases are large and have multiple polarity reversals. These characteristics, especially the large transverse energy, are diagnostic of either a dipping layer or anisotropy. We do not think the dipping layer explanation works here because the large amplitudes and similarity of timing of the *Ps* phase at stations tens of kilometers apart would require a coincidence of multiple steeply dipping interfaces located at about the same depth beneath each station. We consider this scenario geologically unreasonable. A decidedly more likely explanation is that the variations are due to *P–SH* conversions produced at the top of the APMB by seismic anisotropy (LEVIN and PARK, 1997, 1998).

Just as importantly, the combined data clearly show that the receiver functions at stations UYUN and OLLA are quite different, with considerably less azimuthal variations and transverse energy (Fig. 5b). Station OLLA, on the northern edge of the APVC, is within a few kilometers of the active Quaternary arc volcano Ollague. While the OLLA data do display negative polarity arrivals, neither the timing nor the amplitude are similar to the large-amplitude *Ps* phase on the other APVC receiver functions. This contrast supports the idea that both the VLVL and the strong anisotropy are features associated with the APVC and not with the arc volcanoes.

Preliminary Anisotropy Model

Hexagonal symmetry anisotropy, also known as transverse isotropy, is characterized by two orthogonal directions that have the same velocity and a third orthogonal direction, the symmetry axis, that is either faster or slower. Following the nomenclature of Levin and Park, if the symmetry axis is the fast axis, then the equal phase velocity surfaces resemble melons; and if the symmetry axis is the slow

▶

Figure 5(a)

Combined teleseismic (dashed) and low-pass filtered local event (solid) receiver functions and stacks for both radial and transverse components for the 5 stations within the APVC. Numbers of events in the stack are shown above each trace. Note the general similarity of the teleseismic and local receiver functions for similar backazimuths. Large-amplitude *Ps* phases are observed at 2–4 s on both components for all 5 stations. On the radial component a large negative polarity *Ps* is followed by a positive polarity phase. Corresponding phases are usually observed on the transverse component. The phases exhibit azimuthal variations in amplitude and timing on the radial component and multiple polarity reversals on the transverse component. These characteristics are diagnostic of tilted-axis hexagonal symmetry anisotropy as described by LEVIN and PARK (1998). The timing lines are based on station LCOL and repeated on the other stations for comparison.

axis, then the equal phase velocity surfaces resemble pumpkins. This leads to "melon" and "pumpkin" models of anisotropy (LEVIN and PARK, 1998). The former is most often associated with lattice-preferred orientation (LPO) of mineral crystals
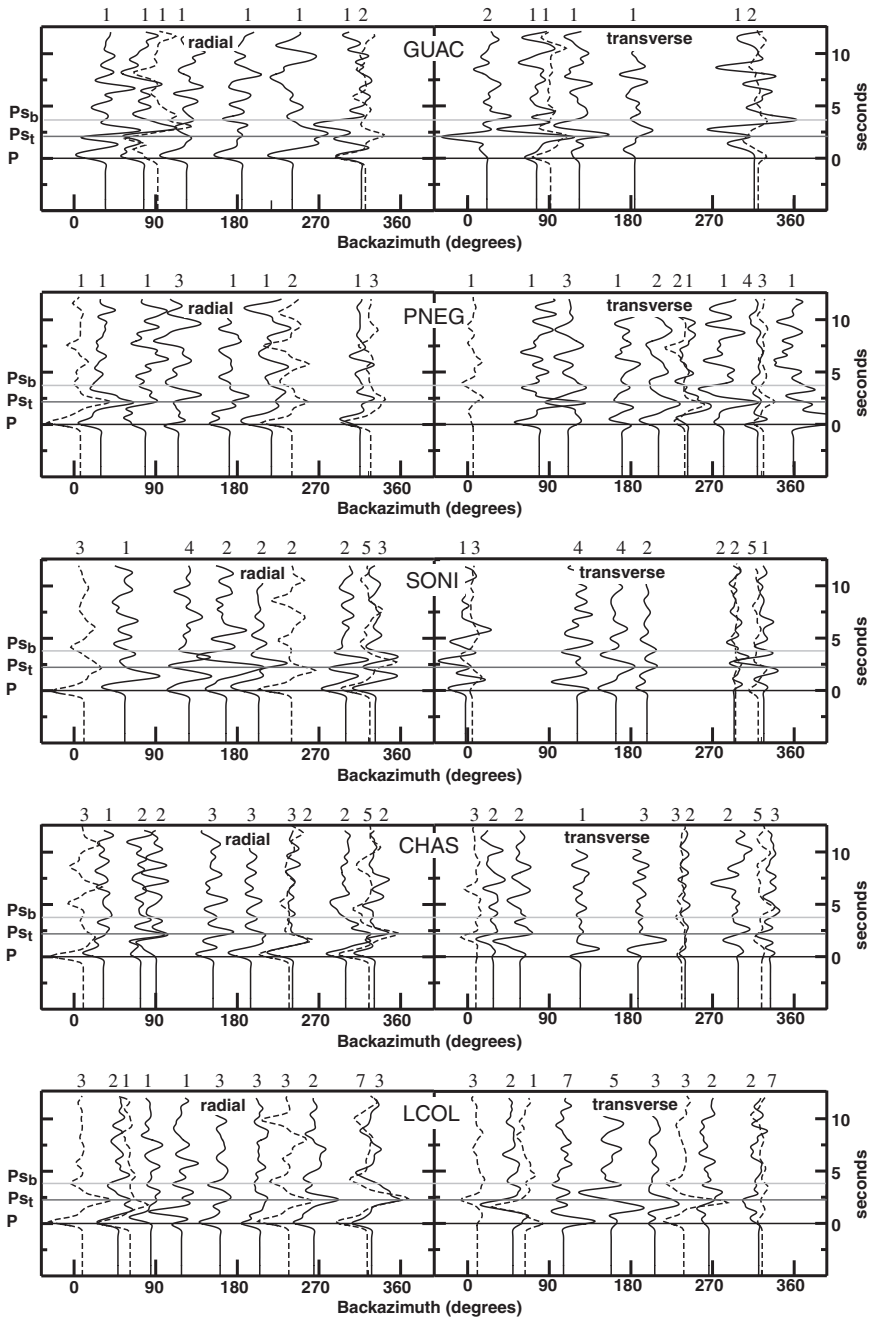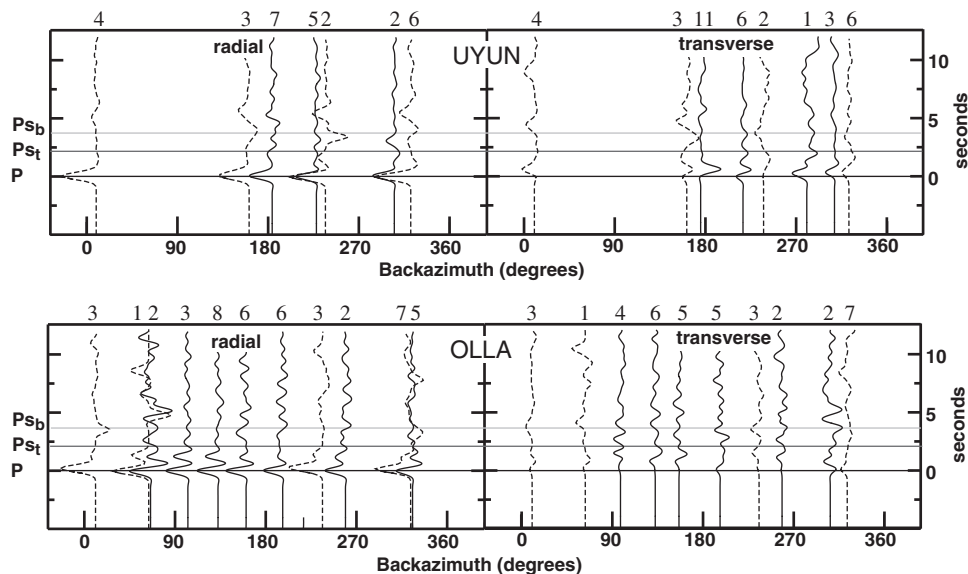
Figure 5(b)

Combined teleseismic (dashed) and low-pass-filtered local event (solid) receiver functions and stacks for both radial and transverse components for stations OLLA and UYUN. Numbers of events in the stack are shown above each trace. Note the lack of similarity of the UYUN and OLLA data to the other APVC stations (Fig. 5a) both in the absence of the large-amplitude *Ps* phases at 2–4 s and less azimuthal variability. The timing lines are based on station LCOL and repeated on the other stations for comparison.

and the latter with aligned cracks or thin layering perpendicular to the symmetry axis. Most previous converted-phase analysis of anisotropy assumed a horizontal axis of symmetry. LEVIN and PARK (1997) formulated the problem with an arbitrary orientation of the symmetry axis and demonstrated that tilted-axis anisotropy in simple flat-layered models can lead to complex waveforms, especially on the transverse component.

We followed the "cookbook" of LEVIN and PARK (1998) to analyze the anisotropy at station Laguna Colorado (LCOL). *P–SH* conversions occur at interfaces where one or both layers are anisotropic. To generate anisotropic features in the *Ps* phase from the top of the APMB, the anisotropy can be in the upper crust, in the low-velocity layer, or in both. The presence of initial *P*-wave energy on the transverse receiver functions is diagnostic of upper-crustal anisotropy. Consequently we first concentrated on this case, assuming the rest of the crust is isotropic. The effect of upper-crustal anisotropy is to "split" the *Ps* phase from the top of the low-velocity zone, generating two phases with variable amplitudes on the radial component and with multiple polarity reversals on the transverse component (Fig. 6, top). The *Ps* phase from the bottom of the low-velocity zone is not split but exhibits significant azimuthal timing perturbations and develops an interference
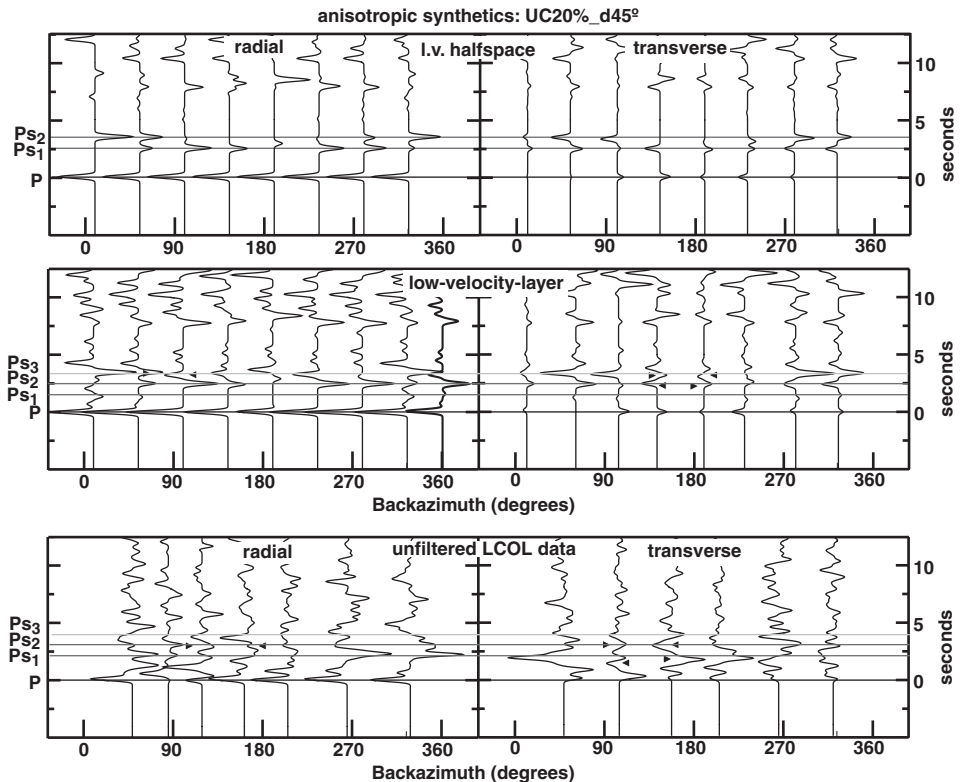
Figure 6

Top panel is Park-Levin synthetic receiver functions for a layer with 20% peak-to-peak "pumpkin" style anisotropy with 45° dip over an isotropic low-velocity halfspace. Note how the negative polarity *Ps* phase from the top of the low-velocity halfspace is "split", with variable amplitudes on the radial component and polarity reversals on the transverse component. Second panel shows synthetics for a model with the same 20% upper crust anisotropy but overlying an isotropic low-velocity layer (l*v*l) only 1 km thick. The effect of the bottom of the low-velocity layer is a third *Ps* phase with positive polarity and variable arrival time that interferes in a complicated pattern with the slow "split-*Ps*." An azimuth independent synthetic for a completely isotropic low-velocity layer model is plotted at 360° as a heavy line. The bottom panel shows the unfiltered local earthquake receiver functions at LCOL. Comparison of the data with synthetics indicates that anisotropy can explain several major characteristics of the data that are inconsistent with a purely isotropic model.

pattern with the second "split *Ps*" (Fig. 6, second panel). The net effect is a complicated waveform that varies in both timing and amplitude as a function of backazimuth, which in a general way mimics the behavior of our APVC data.

Based on these initial observations, we computed synthetics for a range of upper-crust anisotropy parameters, varying the amount of *P* and *S* anisotropy and the inclination of the symmetry axis for both "melon" and "pumpkin" anisotropy. On the basis of visual inspection we found a certain class of models that explains some of the specific waveform complexities observed in the LCOL data (Fig. 6, bottom two

panels). These models have "pumpkin-style" *P*- and *S*-wave anisotropy of 20% and a symmetry axis tilt of 45°. The strike direction is not well constrained in these preliminary models. Comparison of the data with the synthetics indicates that ansiotropy of the upper crust can explain three major characteristics of the data that are inconsistent with a purely isotropic model. These characteristics are: 1) on the radial component, the variable amplitude of the *Ps* from the top of the VLVL, and 2) the complexity and changing polarity of the *Ps* from the bottom of the VLVL, and 3) on the transverse component, the presence of large-amplitude bipolarity arrivals. This type of anisotropy could be due to aligned cracks associated with young volcanic features in the APVC (DE SILVA, 1989).

Regional Crustal Structure

An important question is how the VLVL fits within the context of the regional crustal structure. In the past decade a number of international seismological experiments have greatly improved our knowledge of the lithospheric structure of the central Andes (YUAN *et al.*, 2000). The central Andean crust is thick and predominantly felsic in composition (ZANDT *et al.*, 1996). In an E–W cross section the crustal thickness varies from 75 km in the western and eastern Cordillera, to 60–65 km in the central Altiplano, to 40 km in the active Subandean fold and thrust belt (BECK *et al.*, 1996). In a N–S section along the center of the Andes the crustal thickness varies from 60–65 km in the central Altiplano to as thin as ~50 km in the Puna (YUAN *et al.*, 2000). In conjunction with this crustal thinning, the already low bulk crustal seismic velocity also decreases southward. A regionally prevalent crustal low-velocity layer characterizes the central and southern Altiplano, the western flank of the Eastern Cordillera, and the Puna. The top of the VLVL appears to link with the basal detachment of the fold-thrust belt under the Eastern Cordillera (YUAN *et al.*, 2000). This depth may represent the brittle-ductile transition and be the decoupling depth between upper-crustal imbrication and lower-crustal ductile flow. The APMB is apparently localized at this boundary.

On the APVC receiver functions, the large converted waves and multiples from the VLVL effectively hide the Moho *Ps*. To investigate the larger-scale structure we measured interstation surface-wave dispersion and used a stochastic inversion technique to find models that satisfy the data within the error bounds (BAUMONT *et al.*, 2001). Within the APVC the short interstation distances and large lateral velocity variations contributed to substantial errors in the phase velocity measurements. We improved the results greatly by solving simultaneously for the phase velocity and backazimuth (Fig. 7). Significant deviations from the theoretical backazimuth are observed, and accounting for these deviations greatly improved the precision of the phase velocity measurements. The dispersion data cannot resolve a thin VLVL; nonetheless they are sensitive to the total crustal travel time, which is
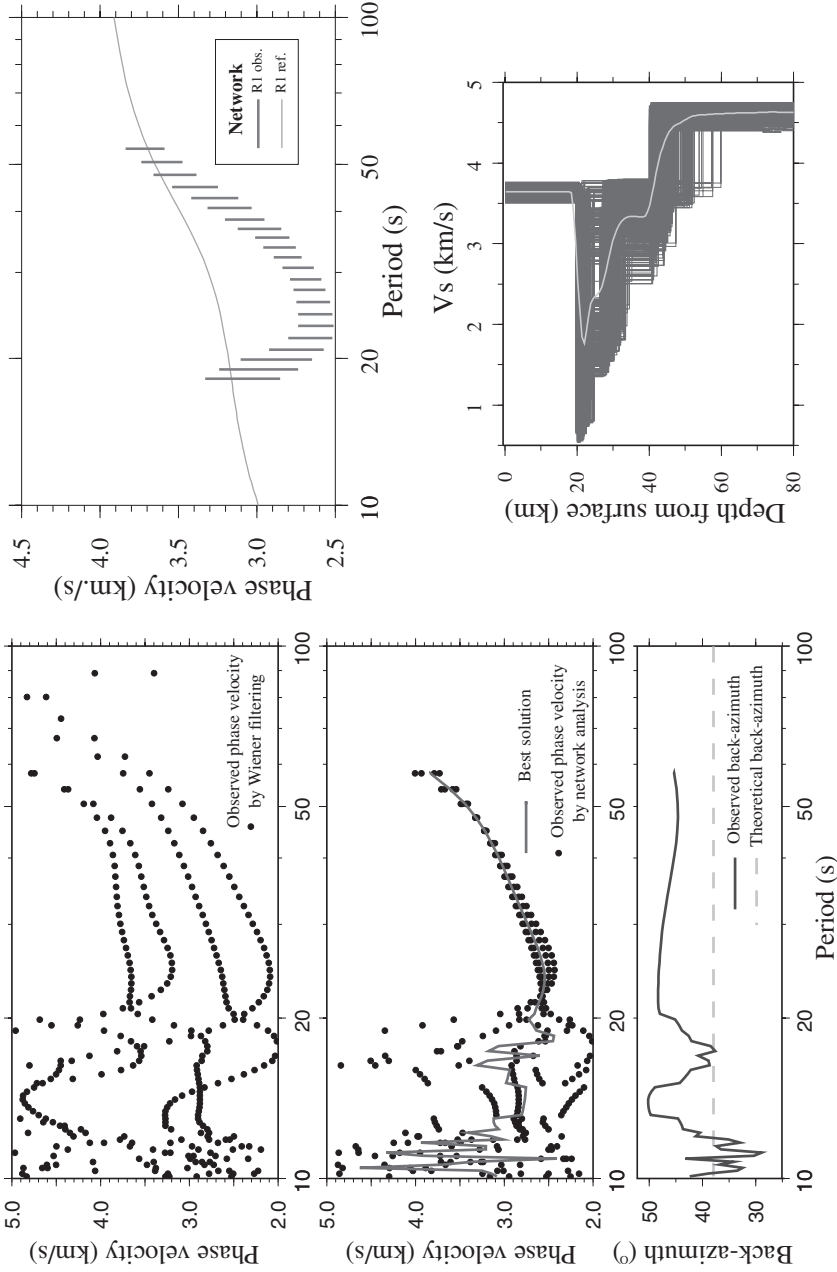
Figure 7

Interstation Rayleigh wave dispersion measurements and inversion results for the region within the APVC network (excluding stations UYUN and OLLA). The left panels show the improvements in the phase velocity measurements by using the APVC network to simultaneously estimate the phase velocity and backazimuth of the surface waves. The final phase velocity measurements and estimated error bounds are shown in the upper right compared with a reference curve for the ZANDT *et al.* (1996) model for the central Altiplano. Lower right is a preliminary model for the APVC from stochastic inversion of the dispersion data with constraints on the 20-km-deep low-velocity layer.

significantly affected by the presence of the VLVL. We ran a series of inversions, including ones with *a priori* constraints on the presence of a thin low-velocity layer based on the receiver functions. The resulting models have extremely low velocities (approaching 0.5 km/s) in the low-velocity layer and Moho depths between 40 and 55 km (Fig. 7). The relatively thin crust is consistent with the regional trends described above, however these preliminary results still require verification.

Magmatism and Tectonics in the Central Andes

The coexistence of a pervasive horizontal sill and inclined aligned cracks might at first seem paradoxical in light of the local stress field. Yet a number of well-documented examples of exactly this situation occur in the present and past geologic record. Two present-day examples from the western United States occur in the Rio Grande Rift near Socorro (New Mexico) and in the Death Valley area of the southern Great Basin (California). In both areas a mid-crustal magma body has been inferred from seismic reflection data, and the dominant tectonic strain field is extensional. The tabular magma bodies are interpreted to lie at a major rheological boundary between a brittle upper crust extending by faulting and a ductile lower crust stretching by penetrative flow and intrusion (DE VOOGD *et al.*, 1988). In Death Valley the upper-crustal faults are planar, with moderate dips of 20° to 35°. In one spectacular seismic reflection record, normal faults can be traced from the inferred magma body at a depth of 15 km to the surface location of a 0.69 Ma basaltic cinder cone (DE VOOGD *et al.*, 1988). Death Valley is also the location of a Miocene pluton that intruded into the mid-crust and which has since been exhumed by extreme extension as part of a core complex. Detailed geologic studies of this pluton and the surrounding rocks convincingly show that entrapment was controlled by a high-strength barrier represented by the brittle-ductile transition (HOLM, 1995).

PARSONS *et al.* (1992) analyzed the mechanics of the emplacement of tabular intrusions into a rheologically stratified lithosphere under extension. The basic idea is that a vertically intruding dike increases the horizontal least principal stress by pushing out on the walls of the host rock. This effect is magnified in a ductile zone, such as the lower crust, where stresses have been partially relaxed by flow. Then subsequent intrusions encounter stress conditions that have been altered to the extent that the local least principal stress has become vertical, favoring horizontal intrusions. The inflation of the horizontal sill in turn increases the vertical maximum principal stress in the overlying brittle layer, favoring extension by either dike intrusion or normal faulting.

All the examples cited above are from extensional regions, yet the APVC is located in one of the largest compressional mountain belts in the world. Perhaps the APVC, with average elevations above 4.4 km, represents a portion of the Andes that has recently undergone the transition from vertical thickening to horizontal,

orogen-parallel extension. It has been postulated that the onset of ignimbrite eruptions may mark this temporal transition in the central Andes (RILLER et al., 1999), while collapse apparently followed ignimbrite volcanism in the western United States (BEST and CHRISTIANSEN, 1991). One interesting possibility was recently published by BOTT (1999), who modeled localized crustal isostasy caused by ductile flow in the lower crust in response to emplacement of a tabular low-density "granitic" body in the upper crust. Both the preliminary indication of crustal thinning within the APVC and geodetic evidence for northward tectonic tilting of the southern Altiplano (BILLS et al., 1994) are possible indications of this type of on-going process. We believe that further study of these crustal sill-like magma bodies will contribute to our understanding of the interplay of tectonics and magmatism in compressional orogens.

Acknowledgments

REFERENCES

AKI, K. (1968), Seismological Evidence for the Existence of Soft Thin Layers in the Upper Mantle under Japan, J. Geophys. Res. 73, 585–594.

AKI, K., CHOUET, B., FEHLER, M., ZANDT, G., KOYANAGI, R., COLP, J., and HAY, R.C. (1978), Seismic Properties of a Shallow Magma Reservoir in Kilauea Iki by Active and Passive Experiments, J. Geophys. Res. 83, 2273–2282.

AKI, K., CHRISTOFFERSSON, A., and HUSEBYE, E. S. (1977), Determination of the Three-dimensional Seismic Structure of the Lithosphere, J. Geophys. Res. 82, 277–296.

BAKER, M.C.W. (1981), The Nature and Distribution of Upper Cenozoic Ignimbrite Centres in the Central Andes, J. Volcanology Geothermal Res. 11, 293–315.

BAUMONT, D., PAUL, A., BECK, S., ZANDT, G., and PEDERSEN, H. (2001), Lithospheric Structure of the Central Andes Based on Surface Wave Dispersion, revised for J. Geophys. Res.

BECK, S. L., ZANDT, G., MYERS, S. C., WALLACE, T. C., SILVER, P. G., and DRAKE, L. (1996), Crustal Thickness Variations in the Central Andes, Geology 24, 407–410.

BEST, M. G. and CHRISTIANSEN, E. H. (1991), Limited Extension During Peak Tertiary Volcanism, Great Basin of Nevada and Utah, J. Geophys. Res. 96, 13509–13528.

BILLS, B. G., DE SILVA, S. L., CURREY, D. R., EMENGER, R. S., LILLQUIST, K. D., DONNELLAN, A., and WORDEN, B. (1994), Hydro-isostatic Deflection and Tectonic Tilting in the Central Andes: Initial Results of a GPS Survey of Lake Minchin Shorelines, Geophys. Res. Lett. 21, 293–296.

BOTT, M. H. P. (1999), *Modeling Local Crustal Isostasy Caused by Ductile Flow in the Lower Crust*, J. Geophys. Res. *104*, 20349–20359.

BROWN, L., CHAPIN, C., SANFORD, A., KAUFMAN, S., and OLIVER, J. (1980), *Deep Structure of the Rio Grande Rift from Seismic Reflection Profiling*, J. Geophys. Res. *85*, 4773–4800.

CAHILL, T. and ISACK, B.L. (1992), *Seismicity and Shape of the Subducted Nazca Plate*, J. Geophys. Res. *97*, 17 503–17 529.

CHMIELOWSKI, J., ZANDT, G., and HABERLAND, C. (1999), *The Central Andean Altiplano–Puna Magma Body*, Geophys. Res. Lett. *26*, 783–786.

CONEY, P. J. (1972), *Cordilleran Tectonics and North American Plate Motion*, Am. J. Sci. *272*, 602–628.

DE SILVA, S. L. (1989), *Altiplano–Puna Volcanic Complex of the Central Andes*, Geology *17*, 1102–1106.

DE SILVA, S. L. and FRANCIS, P. W., *Volcanoes of the Central Andes* (Springer-Verlag, Berlin 1991).

DE SILVA, S. L., SELF, S., FRANCIS, P. W., DRAKE, R. E., and CARLOS, R.R. (1994), *Effusive Silicic Volcanism in the Central Andes: The Chao Dacite and Other Young Lavas of the Altiplano–Puna Volcanic Complex*, J. Geophys. Res. *99*, 17805–17825.

DE VOOGD, B., SERPA, L., and BROWN, L. (1988), *Crustal Extension and Magmatic Processes: COCORP Profiles from the Death Valley and Rio Grande Rift*, Geol. Soc. Am. Bull. *100*, 1550–1567.

ELLSWORTH, W. L. and KOYANAGI, R. Y. (1977), *Three-Dimensional Crust and Mantle Structure of the Kilauea Volcanoe, Hawaii*, J. Geophys. Res. *82*, 5379–5394.

FRANCIS, P., *Volcanoes, a Planetary Perspective* (Clarendon Press, Oxford 1993).

HOLM, D. K. (1995), *Relation of Deformation and Multiple Intrusion in the Death Valley Extended Region, California, with Implications for Magma Entrapment Mechanism*, J. Geophys. Res. *100*, 10495–10505.

IYER, H. M. (1984), *Geophysical Evidence for the Location, Shapes and Sizes, and Internal Structures of Magma Chambers Beneath Regions of Quaternary Volcanism*, Phil. Trans. R. Soc. Lond., *A310*, 473–510.

IYER, H. M., EVANS, J. R., ZANDT, G., STEWART, R. M., COAKLEY, J. M., and ROLOFF, J. N. (1981), *A Deep Low Velocity Body under the Yellowstone Caldera, Wyoming; Delineation Using Teleseismic P-wave Residuals and Tectonic Interpretation: Summary*, Bull. Geol. Soc. Am. *92*, part 1, 792–798.

LEVIN, V. and PARK, J. (1997), *P–SH Conversions in a Flat-layered Medium with Anisotropy of Arbitrary Orientation*, Geophys. J. Int. *131*, 253–266.

LEVIN, V. and PARK, J. (1998), *P-SH Conversions in Layered Media with Hexagonally Symmetric Anisotropy: A Cook Book*, Pure Appl. Geophys. *151*, 669–697.

LIGORRIA, J. P. and AMMON, C. J. (1999), *Iterative Deconvolution and Receiver-function Estimation*, Bull. Seismol. Soc. Am. *89*, 1395–1400.

MAUGHAN, L. L., CHRISTIANSEN, E. H., BEST, M. G., GROMME, C. S., DEINO, A., and TINGEY, D. G. (2002), *The Oligocene Lund Tuff, Great Basin, USA: A Voluminous Monotonous Intermediate*, J. Volcan. Geothermal Res. *113*, 129–157.

PARSONS, T., SLEEP, N. H., and THOMPSON, G. A. (1992), *Host Rock Rheology Controls on the Emplacement of Tabular Intrusions: Implications for Underplating of Extending Crust*, Tectonics *11*, 1348–1356.

RILLER, U., ONCKEN, O., PETRINOVIC, I., and STRECKER, M. (1999), *Late Cenozoic Tectonism and Caldera Formation in the Central Andes*, EOS Trans. AGU *80*, F1061 (1999 Fall AGU Meeting, San Francisco).

ROBERTS, P. M., AKI, K., and Fehler, M. C. (1991), *A Low-Velocity Zone in the Basement Beneath the Valles Caldera, New Mexico*, J. Geophys. Res. *96*, 21,583–21,596.

RUNDLE, J. B. and HILL, D. P. (1988), *The Geophysics of a Restless Caldera – Long Valley, California*, Ann. Rev. Earth Planet. Sci. *16*, 251–271.

SANDFORD, A. R., ALPTEKIN, O., and TOPPOZADA, T. R. (1973), *Use of Reflection Phases on Microearthquake Seismograms to Map an Unusual Discontinuity Beneath the Rio Grande Rift*, Bull. Seismol. Soc. Am. *63*, 2021–2034.

SCHLUE, J. W., ASTER, R. C., and MEYER, R. P. (1996), *A Lower Crustal Extension to a Midcrustal Magma Body in the Rio Grande Rift, New Mexico*, J. Geophys. Res. *101*, 25,283–25,291.

SHEETZ, K. E. and SCHLUE, J. W. (1992), *Inferences for the Socorro Magma Body from Teleseismic Receiver Functions*, Geophys. Res. Lett. *19*, 1867–1870.

STECK, L. K. and PROTHERO, W. A., Jr. (1994), *Crustal Structure Beneath Long Valley Caldera from Modeling Teleseismic P-wave Polarizations and Ps Converted Waves*, J. Geophys. Res. *99*, 6881–6898.

STEEPLES, D. W. and IYER, H. M. (1976), *Low-velocity Zone under Long Valley as Determined from Teleseismic Events*, J. Geophys. Res. *81*, 849–860.

WHITMAN, D., ISACKS, B. L., and KAY, S. M. (1996), *Lithospheric Structure and Along-strike Segmentation of the Central Andean Plateau: Topography, Tectonics, and Timing*, Tectonophysics *259*, 29–40.

YUAN, X., SOBOLEV, S. V., KIND, R., ONCKEN, O., and the ANDES SEISMOLOGY GROUP (2000), *Subduction and Collision Processes in the Central Andes Constrained by Converted Seismic Phases*, Nature *408*, 958–961.

ZANDT, G. and FURLONG, K. P. (1982*), Evolution and Thickness of the Lithosphere Beneath Coastal California*, Geology *10*, 376–381.

ZANDT, G., MYERS, S. C., and WALLACE, T. C. (1995), *Crust and Mantle Structure Across the Basin and Range-Colorado Plateau Boundary at 37°N Latitude and Implications for Cenozoic Extensional Mechanism*, J. Geophys. Res. *100*, 10 529–10 548.

ZANDT, G., BECK, S. L., RUPPERT, S. R., AMMON, C. J., ROCK, D., MINAYA, E., WALLACE, T. C., and SILVER, P. G. (1996), *Anomalous Crust of the Bolivian Altiplano, Central Andes: Constraints from Broadband Regional Seismic Waveforms*, Geophys. Res. Lett. *23*, 1159–1162.

To access this journal online:
http://www.birkhauser.ch